Supplement of Atmos. Chem. Phys., 15, 11311–11326, 2015
http://www.atmos-chem-phys.net/15/11311/2015/
doi:10.5194/acp-15-11311-2015-supplement

Atmospheric Chemistry and Physics Open Access

Supplement of

Investigating the discrepancy between wet-suspension- and dry-dispersion-derived ice nucleation efficiency of mineral particles

C. Emersic et al.

Correspondence to: P. J. Connolly (p.connolly@man.ac.uk)

Supplementary Material

Background experiments without any added mineral particles are shown in Figures S1 and S2. These show that a cloud of supercooled drops form on the aerosol partilces present and that these aerosol particles are not good ice nuclei since very few ice crystals are counted.

Similar plots are shown in Figs. S3 and S4, but for kaolinite at $-19\,^{\circ}\mathrm{C}$ and $-25\,^{\circ}\mathrm{C}$ respectively. In Fig. S3 (middle plot) a cloud of droplets forms for ~ 50 seconds before evaporating to leave an ice cloud. It is more difficult to see from the CDP data that the ice cloud nucleates after the drops form, because the optical sizes of the ice crystals overlap with the optical sizes of the largest kaolinite particles; nevertheless the 3V-CPI data indicated that this was the case (not shown). The bottom plot of Fig. S3 shows that the 3V-CPI derived ice crystal concentration (dotted blue line) is about a factor of two smaller than the particles larger than $20\,\mu\mathrm{m}$ from the CDP (and those larger than $20\,\mu\mathrm{m}$ from the 3V-CPI, solid and dashed blue lines); this is because some of the ice crystals are too small to be able to unequivocally classify them as ice crystals on their shape alone, so we slightly underestimate the ice concentration here.

Figure S4 middle shows that the kaolinite particles nucleate ice in the absence of a cloud of droplets. In fact, the droplets are too small to see with the CDP: the humidity in the chamber was close, and likely above water saturation. The drops are not visible because the Bergeron-Findeison process acts rapidly in this experiment, leaving the drops with little time to grow. The drop mode became more visible with repeat experiments (not shown): (a) because the particle concentration was diluted and (b) because the largest, most IN active particles were used up, which enabled the drops to grow to larger sizes. As for the experiment at higher temperature the 3V-CPI derived ice crystal concentration was below that of the concentrations that were derived on size alone from the CDP and 3V-CPI (solid blue and dashed blue lines respectively). Again this is because the particle sizes were often too small to unequivocally classify them as ice; hence, we classified the ice based on size for these runs (blue lines).

Finally, we have similar plots for the NX-illite sample in Figs. S5 and S6. In Fig. S5 (top) we see that the initial temperature was $-15\,^{\circ}\mathrm{C}$, which decreased to $\sim -23\,^{\circ}\mathrm{C}$ throughout the experiment. The middle plot shows that the droplet mode was of fairly long duration, lasting up to $\sim 300\,\mathrm{s}$ and that there were relatively few ice crystals (as noted from the few speckles above $20\,\mu\mathrm{m}$ in size). The 3V-CPI and CDP derived ice concentrations agree reasonably well in this case; however, the concentration of particles larger than $20\,\mu\mathrm{m}$ as measured with the 3V-CPI is larger than those larger than $20\,\mu\mathrm{m}$ measured with the CDP. The reason for this is that the 3V-CPI has a tendency to over estimate the size of the drops when they are out of focus. Drop concentrations were $\sim 2000\,\mathrm{cm}^{-3}$.

For NX-illite at $-25\,^{\circ}\mathrm{C}$ in Fig. S6 the picture is similar to K-feldspar and kaolinite at the lower temperatures. There is no visible drop mode and the ice crystal concentration inferred from the 3V-CPI images is lower than those inferred from the CDP and 3V-CPI on size alone (bottom plot). The drop mode was visible in later expansions, when the most efficient ice nuclei had been used up and thus removed from the chamber (not shown). The reason the 3V-CPI derived ice crystal concentrations were smaller than the CDP and 3V-CPI concentrations based on size is again due to the ice crystals not developing distinct facets because there are many of them; hence, for these experiments we classified the ice on size alone (blue lines). It is noteworthy that drop concentrations were $\sim 500\,\mathrm{cm}^{-3}$, which is lower than the aerosol by a factor of ~ 3. We suspect that NX-illite, because of its high specific surface area and heteorgeneity, is less effective as a cloud condensation nucleus (CCN) than the other samples, which may be explained by NX-illite having a different adsorption isotherm (e.g. Kumar et al., 2008) in comparison to the other samples.

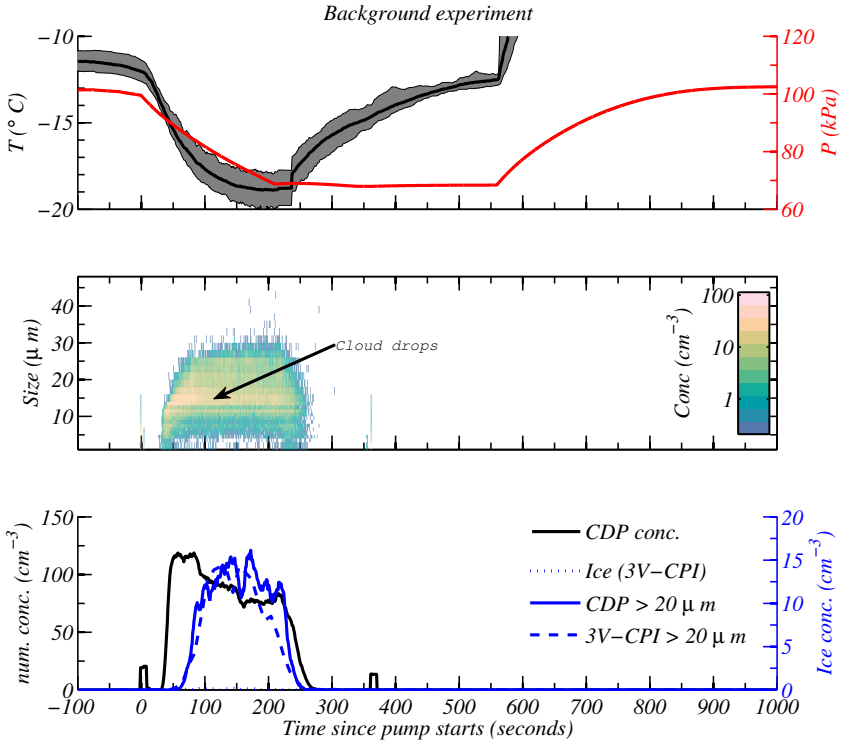

Figure S1. Background experiment at −12 °C before the addition of mineral particles. Top shows the temperature in the chamber (black line, left axis) and the pressure (red line, right axis). The black line is the mean of temperature probes, while the grey shading demarks the range in measured temperatures across all probes. Middle plot shows the size distribution as measured with the CDP instrument. Bottom plot shows: (1) the drop concentration measured with the CDP (black line, left axis); (2) the concentration of particles larger than 20 microns diameter (solid blue line, right axis); (3) the ice crystal concentration measured with the 3V-CPI (dotted blue line, right axis); (4) the concentration of particles larger than 20 microns with the 3V-CPI (dashed blue line, right axis).

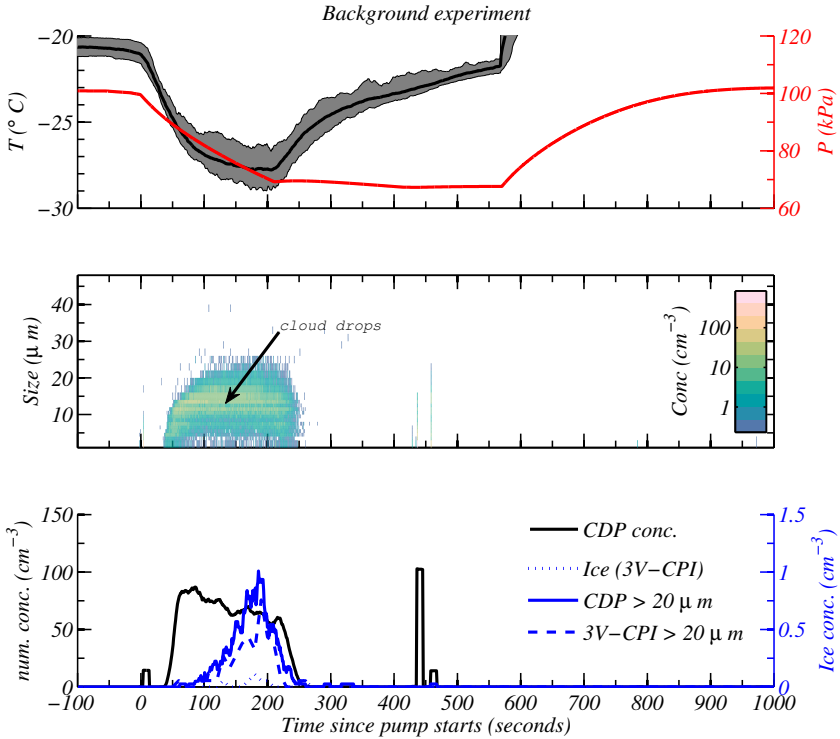

Figure S2. Same as Figure S1, but for a background experiment at −21 °C before the addition of mineral particles.

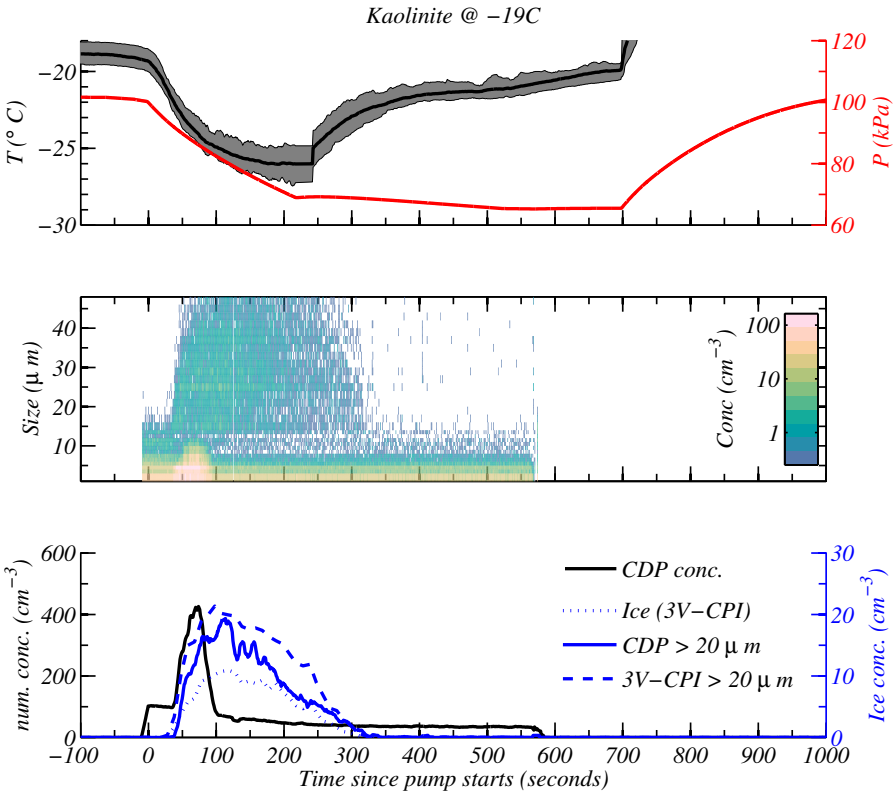

Figure S3. Same as Fig. 2, but for kaolinite at −19 °C.

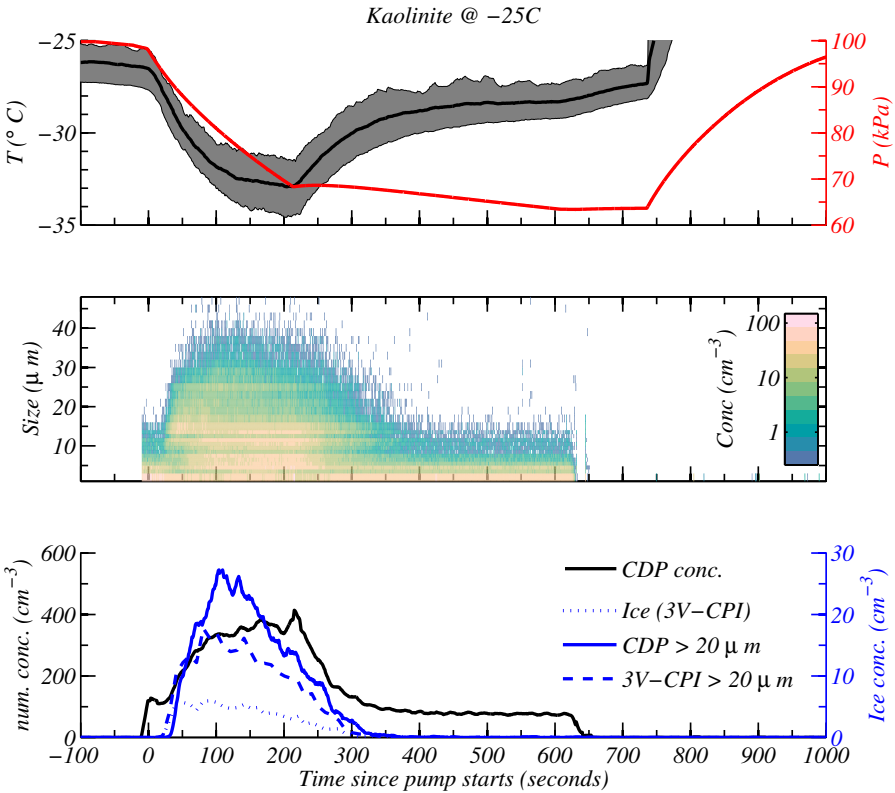

Figure S4. Same as Fig. 2, but for kaolinite at −25 °C.

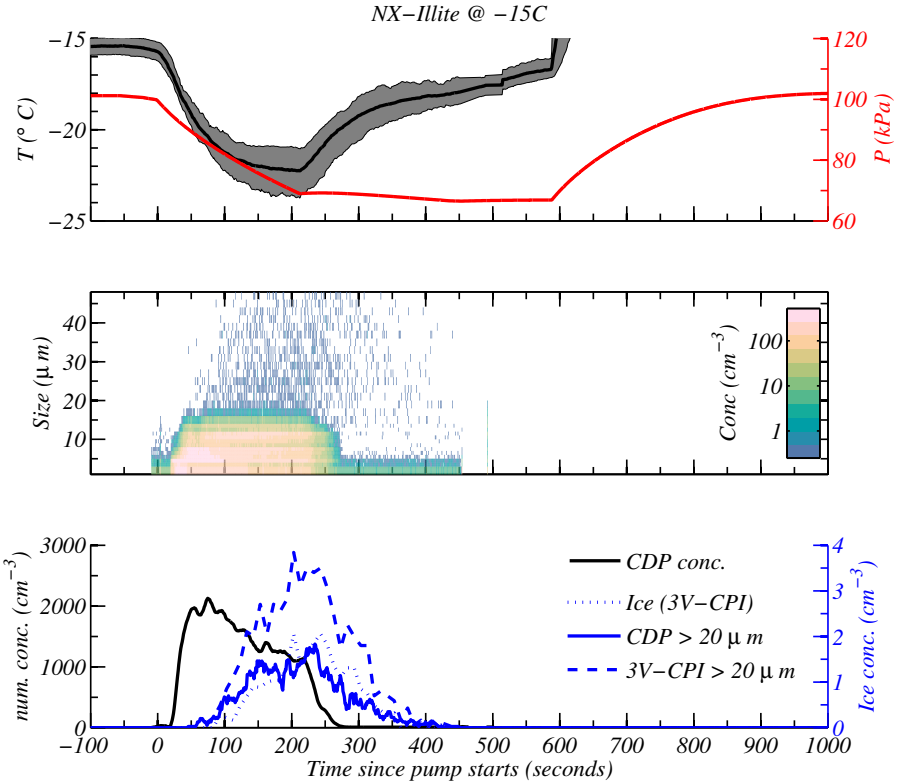

Figure S5. Same as Fig. 2, but for illite at −15 °C.

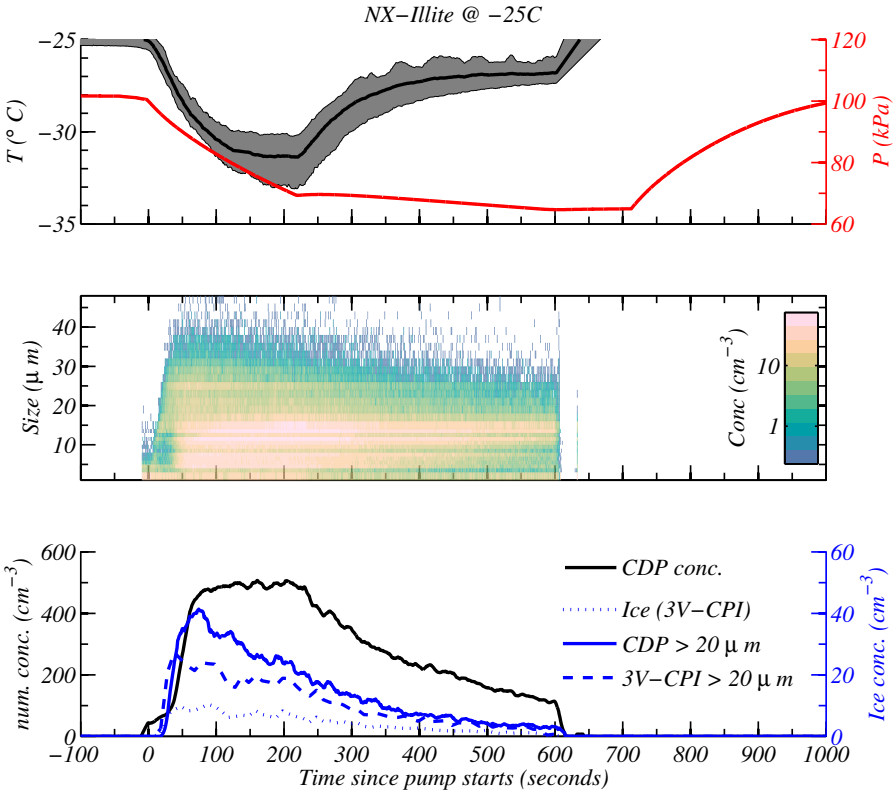
NX−Illite @ −25C
T (° C)
−25
−30
−35
P (kPa)
120
100
80
60
Size (μ m)
40
30
20
10
Conc (cm^−3)
10
1
num. conc. (cm^−3)
600
400
200
0
Ice conc. (cm^−3)
60
40
20
0
CDP conc.
Ice (3V−CPI)
CDP > 20 μ m
3V−CPI > 20 μ m
−100
0
100
200
300
400
500
600
700
800
900
1000
Time since pump starts (seconds)

Figure S6. Same as Fig. 2, but for illite at $-25\,^{\circ}\mathrm{C}$.

References

Kumar, P., Sokolik, I. N., and Nenes, A.: Parameterization of cloud droplet formation for global and regional models: including adsorption activation from insoluble CCN, Atmos. Chem. Phys., 9, 2517–2532, doi:10.5194/acp-9-2517-2009, 2009.